

Viscoelastic subdiffusion in random Gaussian potentials

Igor Goychuk^{1,*}

¹*Institute of Physics and Astronomy, University of Potsdam,
Karl-Liebknecht-Str. 24/25, 14476 Potsdam-Golm, Germany*

(Dated: October 3, 2018)

Viscoelastic subdiffusion governed by a fractional Langevin equation is studied numerically in stationary random Gaussian potentials with decaying spatial correlations. This anomalous diffusion is archetypal for living cells, where cytoplasm is known to be viscoelastic and spatial disorder emerges also naturally. Two type of potential correlations are studied: exponentially-decaying (Ornstein-Uhlenbeck process in space) and algebraically-decaying with an infinite correlation length. It is shown that for a relatively small disorder strength in units of thermal energy (several $k_B T$) viscoelastic subdiffusion in the ensemble sense easily overcomes the potential disorder and asymptotically is not distinguishable from the free-space subdiffusion. However, such subdiffusion on the level of single-trajectory averages still exhibits transiently a characteristic scatter featuring weak ergodicity breaking. With an increase of disorder strength to $5 \div 10 k_B T$, a very long regime of logarithmic Sinai-like diffusion emerges. Long correlations in the potentials fluctuations make such a transient regime essentially longer, but faster in the absolute terms. This nominally ultraslow Sinai diffusion is, however, not dramatically slower than the free-space viscoelastic subdiffusion, in the absolute terms, on the ensemble level. It can transiently be even faster. The explanation of this paradoxical phenomenon is provided. On the level of single-trajectories, such disorder-obstructed persistent viscoelastic subdiffusion is always slower and exhibits a strong scatter in single-trajectory averages.

PACS numbers: 05.40.-a, 82.20.Wt, 87.10.Mn, 87.15.Vv, 87.15.hj

I. INTRODUCTION

Research field of anomalous diffusion and transport [1–11] currently flourishes getting ever more experimental support and manifestations in such diverse research areas as transport processes in living cells and polymeric solutions [12–39], colloidal systems [12, 15, 40, 41], dust plasmas [42], organic photoconductors [43], conformational diffusion in proteins [44–51], self-diffusion in lipid bilayers [52–54], diffusion of proteins on DNA strands [55], to name just a few. It remains at the same time rather controversial because the same phenomena are often described by looking similar but in fact incompatible theories [10, 56], such as continuous time random walks (CTRWs) with a divergent mean residence time in local traps [1–5, 8] *vs.* generalized Langevin dynamics with sub-Ohmic memory friction [10, 57–60]. Different theories of fractional diffusion and transport can indeed look at the first very similar [56]. However, a deeper analysis reveals immediately some profound differences on the fundamental level of e.g. ergodic *vs.* (weakly) non-ergodic behavior [7, 11], nonlinear diffusion in tilted periodic potentials [10, 56, 60, 61], or response to external periodic time modulations [10, 62–66].

On a fundamental level of statistical description, two theoretical approaches are especially important in view of their profound dynamical origin. These are: (1) one based on the Bogolyubov-Ford-Kac-Mazur-Kubo-Zwanzig [67–70] generalized Langevin equation (GLE)

with an algebraically decaying memory [10, 58, 60, 71–73], and (2) normal, memory-less Langevin diffusion in random potentials [3, 6]. Starting from classical works by Bogolyubov [67], Ford, Kac, and Mazur [68], Zwanzig [70] GLE has repeatedly been derived [10, 57, 59, 74, 75] from a fully dynamical system, where the environment is modeled by a large system of harmonic oscillators which form a thermal bath. The only non-dynamical element, which enters this theory, is that the initial positions and momenta of those oscillators are canonically distributed at a given fixed temperature. In this respect, this dynamical theory of Brownian motion presents a precursor and companion of molecular dynamics [76, 77], in a very simplified, model fashion. It is also easy to generalize towards quantum-mechanical Brownian motion [57, 75, 78, 79] anomalous diffusion aspects of which remain still largely unexplored, and to nonlinear models of coupling between the Brownian particle and its linear environment [57, 74]. The influence of environment in this approach is fully characterized by its spectral density [57, 75, 79], $J(\omega)$, which is customarily classified by its low-frequency behavior, $J(\omega) \propto \omega^\alpha$, as Ohmic ($\alpha = 1$), sub-Ohmic ($0 < \alpha < 1$) and super-Ohmic ($\alpha > 1$) [57]. Within a singular bath model with unrestricted energy spectrum and in neglecting quantum effects, the Ohmic model leads exactly [57] to the standard Langevin equation with Stokes friction and thermal white Gaussian noise, which are related by the second fluctuation-dissipation theorem (FDT) established by Kubo [69] also for friction with memory. By the same token, sub-Ohmic model leads to a subdiffusive fractional Langevin equation (FLE) [10, 58, 59, 72, 73, 80], which is a GLE with an algebraically decaying memory fric-

* igoychuk@uni-potsdam.de

tion that can be abbreviated using Caputo time fractional derivative [81, 82]. The entering it thermal fractional Gaussian noise (fGn) [83] is related to the memory friction by the Kubo's second FDT. FLE yields subdiffusion with a sublinear growth of the particles position variance, $\langle \delta x^2(t) \rangle \propto t^\alpha$ [10, 57]. This model and its further generalizations emerge naturally in the context of anomalous diffusion in complex viscoelastic media such as complex liquids, including dense polymeric solutions, dust plasmas, colloids, etc., with a prominent application to anomalous diffusion in cytosol of biological cells, as well as in intrinsic conformational dynamics of proteins. Likewise, the super-Ohmic model with $1 < \alpha < 2$ leads to a superdiffusive FLE with a sign-changing and mostly negative memory kernel [10, 80, 84] whose integral is always positive and tends to zero with the upper limit of integration (vanishing integral friction), and whose absolute value also decays algebraically slow to zero asymptotically. This memory friction is also related to the corresponding anti-persistent thermal fGn by the FDT. For example, it can correspond to hydrodynamic memory effects by Boussinesq and Basset [85] leading to long tails in the velocity autocorrelation function of Brownian particles even in simple fluids [10, 77, 80, 84]. Experimental manifestations of such hydrodynamic effects for Brownian particles were found quite recently [86, 87]. This approach naturally provides a dynamical underpinning and justification of the mathematical model of fractional Brownian motion (fBm) by Kolmogorov [88], Mandelbrot and van Ness [83] within the FLE description upon neglecting the inertial effects. This dynamical origin and consistency with thermodynamics and equilibrium statistical physics for undriven dynamics establish supremacy of this approach over many others in the field of anomalous diffusion [10].

One of special advantages of the GLE approach is that it allows to study nonlinear anomalous dynamics in multistable potentials or force-fields which can be externally imposed. For example, such bistable dynamics was studied in [60] with a prominent result that the residence time distributions (RTDs) in the potential wells are of the stretched exponential type. In fact, no genuine rate description is possible, even though the most probable value of the logarithmically-transformed inverse of the mean residence times is given [10, 50, 60] by the Grote-Hynes rate of the non-Markovian rate theory [89, 90]. With an increase of the barrier height over $10 k_B T$ the rate description is, however, gradually restored with RTDs approaching exponential distributions. Nevertheless, the spectral analysis of bistable fluctuations reveals a $1/f$ noise feature at small frequencies [60], which reflects the fact that relaxation of well populations in the long time limit always follows a power law. This is due to the presence of slow medium fluctuations such that *relatively fast* escape events can occur from one potential well to another on the background of such very sluggish, quasi-static fluctuations of the environment. Such fluctuations induce a dynamic, temporal symmetry breaking even in a

completely symmetric (on the Hamiltonian level) bistable dynamics what makes the whole setup of this anomalous rate problem very different from the classical rate theory. The latter one assumes that the intrawell relaxation occurs much faster than the escape events. This basic assumption is fundamentally broken for viscoelastic subdiffusive escape, where the slow modes of viscoelastic environment result into a time-modulation of the escape rate formed by the *relatively* faster relaxation modes. This leads to break down of an effective rate description [10, 60], even if RTDs in metastable wells have all the moments finite.

Next, the discussed subdiffusion in a washboard potential was shown to be insensitive asymptotically to the presence of potential [60]. It approaches gradually a free-subdiffusion limit [10, 56, 60] for any barrier height. This astounding feature, which is in a sharp contrast with both the intuition and well-known results on normal diffusion in washboard potentials [90], as well as fractional Fokker-Planck subdiffusion in such potentials [61], was also demonstrated for diffusion and transport in other tilted periodic potentials including ratchets potentials with broken space inversion symmetry [10, 56]. Within a quantum-mechanical setting, it has been proven exactly, however, for strictly sinusoidal potentials only [57, 91]. In fact, it is not caused by quantum-mechanical effects at all, as one might possibly believe, and it is not restricted by sinusoidal potentials only [10]. In this respect, it is also important to mention that free viscoelastic diffusion is ergodic: the ensemble and single-trajectory averages coincide [60], in a sharp contrast e.g. with continuous time random walk (CTRW) semi-Markovian subdiffusion [11, 92, 93]. However, imposing a periodic potential makes it transiently non-ergodic [60].

For the mentioned reasons, the emergence of a directed transport in such unbiased on averaged, time-modulated potentials [94], or anomalous diffusion ratchet effect, is a highly nontrivial phenomenon. It emerges because the transient to the discussed asymptotics in the case of static potentials can last very long for sufficiently large potential amplitudes. Such a rocking viscoelastic ratchet demonstrating anomalously slow directed transport or sub-current has first been studied in Ref. [95]. Later on, it has been shown that the corresponding subtransport, which is not characterized by velocity, but rather sub-velocity, is optimized when the frequency of external driving matches the inverse mean residence time (MRT) in the potential wells [96]. This leads to a genuine non-Markovian stochastic resonance effect, when the driving-induced sub-transport is getting optimized at some optimal temperature [96]. Stochastic energetics of such ratchets has been studied in Refs. [97, 98]. Flashing subdiffusive ratchets with on-off potential fluctuations were introduced in Ref. [99], where also many further surprising features have been demonstrated. These include: (i) genuine nonlinear resonance and synchronization due to the presence of inertial effects, which, astoundingly, co-exist with anomalous sub-transport, and

(ii) a resonance-like control of the rectified sub-current direction by the driving frequency. Remarkably, diffusional spread is only weakly affected by driving and the quality of sub-transport, as characterized by a generalized Peclet number, can be very high. These flashing viscoelastic ratchets have further been generalized to model kinesin molecular motors operating in viscoelastic environment of living cells, and their stochastic energetics has also been studied [34]. It has been shown that such model motors can realize both normal and anomalous transport with a remarkable thermodynamic efficiency reminiscent of real molecular motors. It allowed to solve the puzzle of how a very efficient transport of large submicron cargoes, which extremely slow subdiffuse in the absence of motors [22, 33], is possible by the motors, which continue to work remarkably efficient despite subdiffusive obstructions introduced by molecularly crowded cytosol. This approach to anomalous diffusion and transport has proven its utility in producing a number of very surprising, important, and experimentally relevant results within the last decade.

Another important approach to anomalous diffusion is based on normal diffusion in random potentials [3, 5, 6]. Such random potentials naturally emerge in inhomogeneous disordered materials, including also viscoelastic cytosol of living cells. This is also a very rich approach. For example, the model of stationary exponentially distributed energy disorder with root-mean-square (rms) amplitude of fluctuations σ leads in a mean-field approximation to CTRW subdiffusion with a power law RTD, $\psi(\tau) \propto \tau^{-1-\alpha}$, $0 < \alpha = k_B T / \sigma < 1$, in local traps [5]. It is featured by divergent mean residence times (MRTs) [1, 2] and is (weakly) nonergodic [7, 21, 92, 93, 100, 101]: The ensemble and trajectory averages are radically different.

However, in stationary Gaussian potentials such diffusion is asymptotically normal for any decaying potential correlations in space, with a prominent result by de Gennes, Bässler, and Zwanzig on the renormalized normal diffusion coefficient, $D_{\text{ren}} = D_0 \exp[-\sigma^2 / (k_B T)^2]$, where D_0 is the potential-free diffusion coefficient [102–105]. The corresponding temperature dependence is customarily measured in disordered materials [106] and the Gaussian model of energy disorder is physically well justified in many cases, e.g. for diffusion of electrons and holes in organic photoconductors [104, 107], colloidal particles in random laser fields [40, 41, 108] and regulatory proteins on DNA tracks [109–113]. However, for a sufficiently strong disorder $\sigma > 2k_B T$ long subdiffusive transients occur on a mesoscale [113–116] with a time-dependent sub-diffusion exponent $\alpha(t) \propto \log(t)$ [117]. For $\sigma > (4 \div 5)k_B T$, this mesoscale subdiffusion can reach even the macroscale [113], and $\alpha(t)$ can be nearly constant for a very long time [113, 117]. Remarkably, in this regime it exhibits the same temperature dependence, $\alpha \propto k_B T / \sigma$, as in the case of exponential disorder, despite a very different physical mechanism [117]. Such transient subdiffusion also exhibits a strong scatter in

single-trajectory averages pointing out on the absence of ergodic self-averaging [113].

Furthermore, if Gaussian potential is non-stationary and presents an unbounded Brownian motion (Wiener process) in space, normal diffusion in such a potential results into the logarithmically slow Sinai diffusion [3, 118], $\langle \delta x^2(t) \rangle \propto \log^a(t)$ with $a = 4$ [3]. If potential presents a fBm in space, a generalized Sinai diffusion with $a \neq 4$ emerges [119]. Astoundingly, generalized Sinai diffusion emerges also transiently in stationary correlated Gaussian potentials for a sufficiently strong disorder, $\sigma > 5k_B T$, as it has been shown recently for four different models of disorder correlations in Ref. [117]. In this recent work, also the genuine mechanism of the discussed transient subdiffusion has been clarified using a scaling theory argumentation.

Viscoelastic subdiffusion in random potentials presents currently a practically unexplored topic in spite of its obvious relevance for e.g. diffusion processes in cytosol of living cells, and other inhomogeneous viscoelastic media. Only in a parabolic weakly corrugated trapping potential such a diffusion was partially addressed recently [120]. This is the main purpose of this paper to do the first systematic study of viscoelastic subdiffusion in stationary Gaussian potentials with decaying correlations. We shall investigate two such models: (i) with exponentially decaying correlations (Ornstein-Uhlenbeck process in space), and (ii) algebraically decaying correlations possessing no effective correlation length. The rest of the paper is organized as follows. In Sec. II, we formulate the model and the numerical approach. In Sec. III, we present the main results and their discussion. Finally, in Sec. IV, the main conclusions will be drawn.

II. MODEL AND NUMERICAL APPROACH

We consider one-dimensional viscoelastic subdiffusion governed by the following overdamped subdiffusive FLE [10, 50, 98]

$$\eta_0 \frac{dx}{dt} + \eta_\alpha \frac{d^\alpha x}{dt^\alpha} = f(x) + \xi_0(t) + \xi_\alpha(t). \quad (1)$$

The particles are moving in a random potential $U(x)$ yielding static random force $f(x) = -dU(x)/dx$, and are also subjected to stochastic thermal Gaussian forces $\xi_0(t)$ and $\xi_\alpha(t)$, as well as memoryless Stokes friction with the friction coefficient η_0 and a friction with memory or frequency-dependent friction, which is characterized by the fractional friction coefficient η_α and the fractional Caputo time derivative of the coordinate, $\frac{d^\alpha x}{dt^\alpha} := \int_0^t (t-t')^{-\alpha} \dot{x}(t') dt' / \Gamma(1-\alpha)$ [81, 82]. This latter one is used to short-hand a general frictional force with memory in GLE, $f_{\text{mem}}(t) = -\int_0^t \eta(t-t') \dot{x}(t') dt'$ for a particular case of power-law decaying memory kernel $\eta(t) = \eta_\alpha t^{-\alpha} / \Gamma(1-\alpha)$. Here, $\Gamma(x)$ is familiar Gamma-

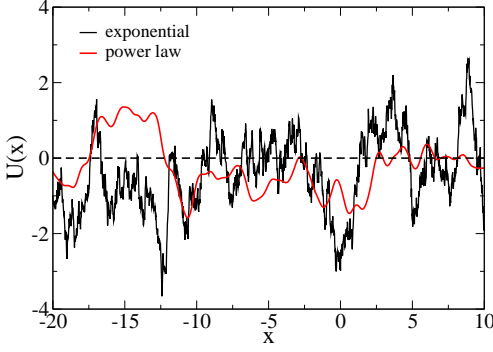


FIG. 1. (Color online) Realizations of random potentials (energy in units of σ , and coordinate in units of λ) for exponential and power law correlations. The lattice grid size is $\Delta x = 0.02$. In the case of power-law correlations, $\gamma = 0.8$.

function and $0 < \alpha < 1$. Thermal noises and the corresponding frictional parts are related by the FDT relations $\langle \xi_0(t)\xi_0(t') \rangle = 2k_B T \eta_0 \delta(t - t')$, and $\langle \xi_\alpha(t)\xi_\alpha(t') \rangle = k_B T \eta_\alpha |t - t'|^{-\alpha} / \Gamma(1 - \alpha)$, correspondingly, which ensure statistical equilibrium description in the absence of driving forces [69]. Hence, $\xi_\alpha(t)$ is a fractional Gaussian noise, which also like white Gaussian noise $\xi_0(t)$ is a singular stochastic process with infinite variance. In the language of spectral bath functions, this description corresponds to $J(\omega) = \eta_0 \omega + \eta_\alpha \omega^\alpha$, i.e. a mixture of Ohmic and sub-Ohmic thermal baths [57]. In the case of cytosol or complex polymeric liquids, the Stokes friction accounts for the water component of solution, whereas the memory friction is caused by various dissolved polymers forming e.g. actin meshwork. We neglect inertial effects in anomalous dynamics, which can also be easily included [10, 60], because we wish to arrive at a largest possible time scale accessible in numerical simulations and very often such effects can indeed be neglected on physical grounds, see Appendix A for a justification.

The solution of Eq. (1) for free subdiffusion, $f(x) = 0$, yields [98]

$$\langle \delta x^2(t) \rangle = 2D_0 t E_{1-\alpha, 2}[-(t/\tau_0)^{1-\alpha}], \quad (2)$$

where $E_{a,b}(z) := \sum_{n=0}^{\infty} z^n / \Gamma(an+b)$ is generalized Mittag-Leffler function, $D_0 = k_B T / \eta_0$ is a normal diffusion coefficient, and $\tau_0 = (\eta_0 / \eta_\alpha)^{1/(1-\alpha)}$ is a transient time constant. Initially, for $t \ll \tau_0$, diffusion is normal, $\langle \delta x^2(t) \rangle \approx 2D_0 t$, and asymptotically, $t \gg \tau_0$, it is anomalously slow, $\langle \delta x^2(t) \rangle \sim 2D_\alpha t^\alpha / \Gamma(1 + \alpha)$, with anomalous diffusion coefficient $D_\alpha = k_B T / \eta_\alpha$. In a particular case of $\alpha = 1/2$, Eq. (2) yields

$$\langle \delta x^2(t) \rangle = 2D_{1/2} \left\{ 2\sqrt{\frac{t}{\pi}} + \sqrt{\tau_0} \left[e^{t/\tau_0} \operatorname{erfc} \left(\sqrt{\frac{t}{\tau_0}} \right) - 1 \right] \right\}, \quad (3)$$

which is used to test numerical solutions below.

We consider stationary zero-mean random Gaussian potentials, which are completely characterized by the normalized autocorrelation function $g(x) = \langle U(x_0 + x)U(x_0) \rangle / \langle U^2(x) \rangle$, and the rms of fluctuations, $\sigma = \langle U^2(x) \rangle^{1/2}$. Two models of correlations are considered: (i) exponential, $g(x) = \exp(-|x|/\lambda)$, and (ii) power law decaying, $g(x) = 1/(1 + x^2/\lambda^2)^{\gamma/2}$. In the first case, λ is the correlation length, $\lambda_{\text{corr}} = \int_0^\infty g(x) dx$, and in the second case $\lambda_{\text{corr}} \rightarrow \infty$, for $0 < \gamma < 1$, as e.g. for diffusion of proteins on biological DNAs [4, 117, 121]. Then, λ is just a scaling parameter, which is convenient to use to scale distance in numerics. Furthermore, the time will be scaled in the units of $\tau_r = (\lambda^2 \eta_\alpha / \sigma)^{1/\alpha}$, $k_B T$ in units of σ , and normal friction coefficient η_0 in units of $\eta_\alpha \tau_r^{1-\alpha}$. Random potentials are generated on a lattice with a grid size $\Delta x \ll \lambda$, using a spectral method as detailed in Ref. [122], which implies use of periodic boundaries with a very large period L . In our numerics we fix $\Delta x = 0.02$, and $L = 2^{19} \approx 10^4$. Examples of random potentials with different correlations are presented in Fig. 1. Notice a very rough character of the potential fluctuations for exponential correlations. There are many minima and maxima present within a correlation length. This is because this is a singular model of correlations. As a matter of fact, the corresponding $\langle f(x) \rangle^{1/2} = \sqrt{2/(\Delta x \lambda)} \sigma$ diverges in the limit of $\Delta x \rightarrow 0$. This is a crucial point: Δx must be finite, on physical grounds in any such singular model [117]. The model of a delta-correlated potential is physically a model with $U(x)$ values uncorrelated on the lattice sites. However, because of continuity of potential it remains correlated between the sites of the lattice, anyway [117]. This is actually the case, where the potential fluctuations have the wildest character, and do not exhibit a *local bias*, which otherwise is *always present* because of correlations. In our numerics we connect the lattice values of potential by parabolic splines, i.e. the potential is locally parabolic and $f(x)$ is piece-wise linear. Notice also that the power-law correlated potential is much smoother and it does not display the discussed singularity in the limit $\Delta x \rightarrow 0$.

A. Numerical approach

Our numerical approach to integrate the FLE dynamics is based on approximation of the power-law memory kernel by a sum of exponentials, $\eta(t) = \sum_{i=1}^N k_i \exp(-\nu_i t)$, i.e. using a Prony series expansion [60, 123] with purely imaginary frequencies, and introduction of a subset of auxiliary variables x_i [60]. Physically, they can be interpreted as coordinates of some auxiliary Brownian quasi-particles modeling viscoelastic Maxwellian modes of the environment and elastically coupled with spring constants k_i to the central Brownian particle [10]. The fractional Gaussian noise $\eta_\alpha(t)$ in this approach is approximated by a sum of Ornstein-

Uhlenbeck processes with autocorrelation times $1/\nu_i$. Very important and even crucial in applications is that this Maxwell-Langevin approach to viscoelastic subdiffusive dynamics allows for a straightforward Markovian embedding [10]:

$$\begin{aligned}\eta_0 \dot{x} &= f(x) - \sum_{i=1}^N k_i (x - x_i) + \sqrt{2k_B T \eta_0} \zeta_0(t), \\ \eta_i \dot{x}_i &= k_i (x - x_i) + \sqrt{2k_B T \eta_i} \zeta_i(t),\end{aligned}\quad (4)$$

where $\zeta_i(t)$ are $N+1$ uncorrelated white Gaussian noises, $\langle \zeta_i(t) \zeta_j(t') \rangle = \delta_{ij} \delta(t-t')$, and η_i are frictional coefficients of auxiliary Brownian particles. This Markovian dynamics in the space of $N+1$ dimensions can be propagated using well-established algorithms like stochastic Euler or stochastic Heun methods [124] without principal difficulties, with a well controlled accuracy. By excluding auxiliary variables in Eq. (4) it is easy to show that the resulting GLE for the coordinate x has indeed the memory kernel, which is presented by the above sum of exponentials, and the correlated noise term, which is the sum of corresponding Ornstein-Uhlenbeck processes. This equivalence holds provided that $\eta_i = k_i/\nu_i$, and the initial $x_i(0)$ are randomly distributed so that, $\langle x_i(0) \rangle = x(0)$, $\langle [x_i(0) - x(0)]^2 \rangle = k_B T/k_i$. The considered Markovian embedding is exact, when the memory kernel is exactly the sum of exponentials.

To approximate a power law memory kernel, one chooses a fractal scaling of the relaxation rates $\nu_i = \nu_0/b^{i-1}$, and the corresponding spring constants $k_i = C_\alpha(b) \nu_i^\alpha / \Gamma(1-\alpha) \propto \nu_i^\alpha$, where $C_\alpha(b)$ is some constant, which depends on α and b [5, 10, 60, 125]. Already for a crude decade scaling with $b = 10$, the accuracy of approximation reaches several percents for $\alpha = 0.5$ between two memory cutoffs, $\tau_l = 1/\nu_0$ and $\tau_h = \tau_l b^{N-1}$. This allows for a numerically very efficient approach to integrate FLE [10, 60]. Notice that ν_0 can be chosen somewhat smaller (to avoid numerical instability) than the inverse time step Δt in the numerical simulation, and even $N \sim 10 \div 20$ is typically sufficient in numerical simulations. For an octave scaling with $b = 2$, the accuracy of approximation can be as good as 0.01% [97]. Then, however, one should also increase N accordingly, which provides an extra time burden in the numerics. In any particular case, one should choose the embedding parameters appropriately, considering a trade-off between the numerical accuracy and feasibility of simulations on the required time scale. The accuracy can be controlled by comparison with the exact results like one in Eq. (2), when available.

The whole idea of Markovian embedding is very natural in view of a dynamical origin of GLE dynamics: Instead of considering huge many thermal bath oscillators one replaces them by a handful of overdamped stochastic Brownian oscillators, with a nice physical interpretation in terms of a generalized Maxwell-Langevin theory of viscoelasticity [10]. It can also be related to a temporary network model of polymeric melts and further be phys-

ically justified within an eigen-modes dynamics of polymeric models like Rouse model [126]. However, in the latter case the scaling is different: $\nu_i = \nu_0/i^p$, $k_i \propto \text{const}$ [10, 123], e.g. $p = 2$ for the Rouse model yielding $\alpha = 0.5$. However, the fractal scaling, which we use, is numerically clearly preferable because it requires much smaller embedding dimensions. Indeed, for having the same lowest value of ν_i for M eigen-modes in the second polymeric scaling as for N auxiliary particles in the first fractal scaling one has obviously the following condition: $M^p = b^{N-1}$. From this,

$$M = b^{(N-1)/p}. \quad (5)$$

For $\alpha = 0.5$ and $p = 2$ this would give $M = 10^5$ (!) for $b = 10$ and $N = 11$, which establish a clear supremacy of our choice. The efficiency of the resulting numerical approach has a proven record [10, 34, 60, 95, 97, 99]. Upon a modification, this method can also be used for a Markovian embedding of superdiffusive FLE dynamics [84, 127]. Clearly, it can be also considered as an independent approach to anomalous dynamics without any relation to FLE.

In our simulations below we use for $\alpha = 0.5$, $b = 10$, $\eta_0 = 0.1$, $\nu_0 = 10^3$, $N = 12$, $C_{0.5}(10) = 1.3$, which warrants $3 \div 5\%$ accuracy in numerics. The rms of potential σ is fixed in simulations, whereas temperature varies in units of σ/k_B . The time-step of integration was chosen $\Delta t = 5 \times 10^{-5}$, and the maximal time was $t_{\max} = 2 \times 10^5$. Stochastic Heun method was used with double precision on high-performance graphical processors Tesla K20. In the ensemble trajectory simulations, $n = 10^4$ particles were initially uniformly distributed within $[0, L]$ spatial interval with 10 different potential realizations in each case (10^5 particles in the ensemble averaging). Random potentials were generated as described above, in accordance with [122], and simulations were run with periodic boundary conditions. It took typically about 5 days of computational time for each ensemble-averaged curve presented below. The results were first tested against the exact analytical result in Eq. (3) in the absence of random potential. The numerical results coincide in this case with the analytical result within the width of the plotted curves like in Fig. 2, a in Ref. [60], and especially, Figs. 5, 6 in Ref. [10], Fig. 2 of [97] and inset of Fig. 1 in [98].

III. RESULTS AND DISCUSSION

A. Ensemble averaging

We first concentrate on the ensemble averaging. The results are shown in Fig. 2 for the exponentially decaying correlations in part (a) and for the power-law decaying correlations with $\gamma = 0.8$ in part (b), for several different values of temperature starting from $T = 1$ and ending with $T = 0.1$. The first striking feature for both types of correlations is that random potential practically does not

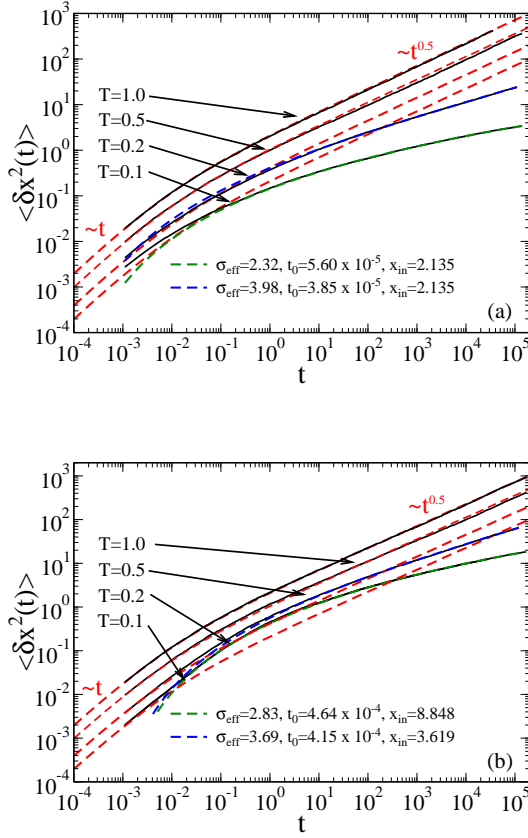


FIG. 2. (Color online) Ensemble-averaged mean squared displacement versus time in units of $\tau_r = (\lambda^2 \eta_\alpha / \sigma)^{1/\alpha}$ for different values of $k_B T$ in units of the disorder strength σ for (a) exponential decay of correlations and (b) power-law decay with $\gamma = 0.8$. The fit of the numerical results (full black lines) is performed for $T = 0.2$ with the expression (7) and for $T = 0.1$ using (6). The fitting parameters are shown in the plot. Dashed red lines depict exact results for free subdiffusion in accordance with Eq. (3): $\alpha = 0.5$, $\eta_0 = 0.1$ and $\tau_0 = 0.01$.

matter for $T = 1$ and the results are not different from the exact result of potential-free subdiffusion depicted by a broken red line in accordance with Eq. (3). This is not a trivial feature at all, even if it could be expected from the earlier results on viscoelastic subdiffusion in periodic potentials [10, 60]. However, intuition says that a combination of slowness caused viscoelastic effects with sluggishness caused by random potential should result into an ultraslow behavior. This intuition is wrong. Very differently from normal diffusion in stationary Gaussian potentials, which asymptotically is (super)-exponentially suppressed by disorder, viscoelastic subdiffusion is not suppressed at all, on the ensemble level, asymptotically. Especially for the exponential correlations this result is very surprising even for $T = 1$, as soon one realizes that in this case the amplitude of potential fluctuations can largely exceed $k_B T$ well within a distance of the correlation length, see in Fig. 1. However, with lowering temperature the influence of potential becomes visible

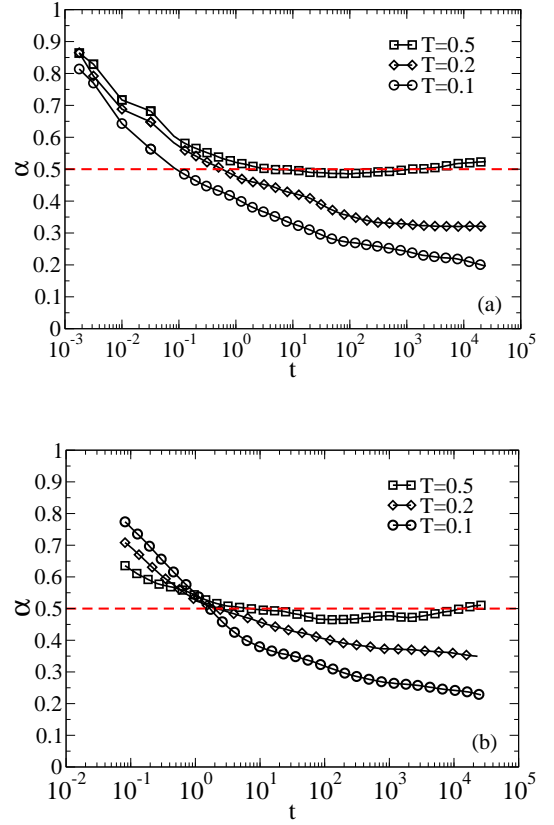


FIG. 3. (Color online) Time-dependent power law exponent $\alpha(t)$ for an assumed subdiffusive law $\langle \delta x^2(t) \rangle \simeq t^{\alpha(t)}$ obtained as the logarithmic derivative of the traces in Fig. 2, for different temperatures in the case of (a) exponential correlations, (b) power law correlations with $\gamma = 0.8$.

already for $T = 0.5$, although the potential-free asymptotics is almost reached at the end point of simulations in Fig. 2, and the influence is really small, barely detectable. For $T = 0.1$, it becomes very distinct, and the corresponding transient regime lasts indeed very long: No slightest signature of an asymptotic regime is even present in Fig. 2 for $T = 0.1$. The corresponding asymptotics is simply impossible to reach numerically. Instead of a power-law subdiffusion, one clearly detects a nominally ultra-slow logarithmic diffusion of the Sinai type:

$$\langle \delta x^2(t) \rangle \approx x_{\text{in}}^2 [(k_B T / \sigma_{\text{eff}}) \ln(t/t_0)]^4 \quad (6)$$

with three fitting parameters: σ_{eff} , x_{in}^2 , and t_0 , two of which can be combined in the only one, $x_{\text{in}}^2 / \sigma_{\text{eff}}^4$, in this case. It describes numerics nicely over about 7 time decades for both types of correlations. For a larger $T = 0.2$, numerics are fitted well by a more complex, yet only three parameters dependence [117]

$$\langle \delta x^2(t) \rangle = x_{\text{in}}^2 \left\{ e^{[(k_B T / \sigma_{\text{eff}}) \ln(t/t_0)]^2} - 1 \right\}^2. \quad (7)$$

It follows from a scaling consideration assuming that the time to travel a certain distance x is defined in an Arrhenius manner by the largest potential barrier met

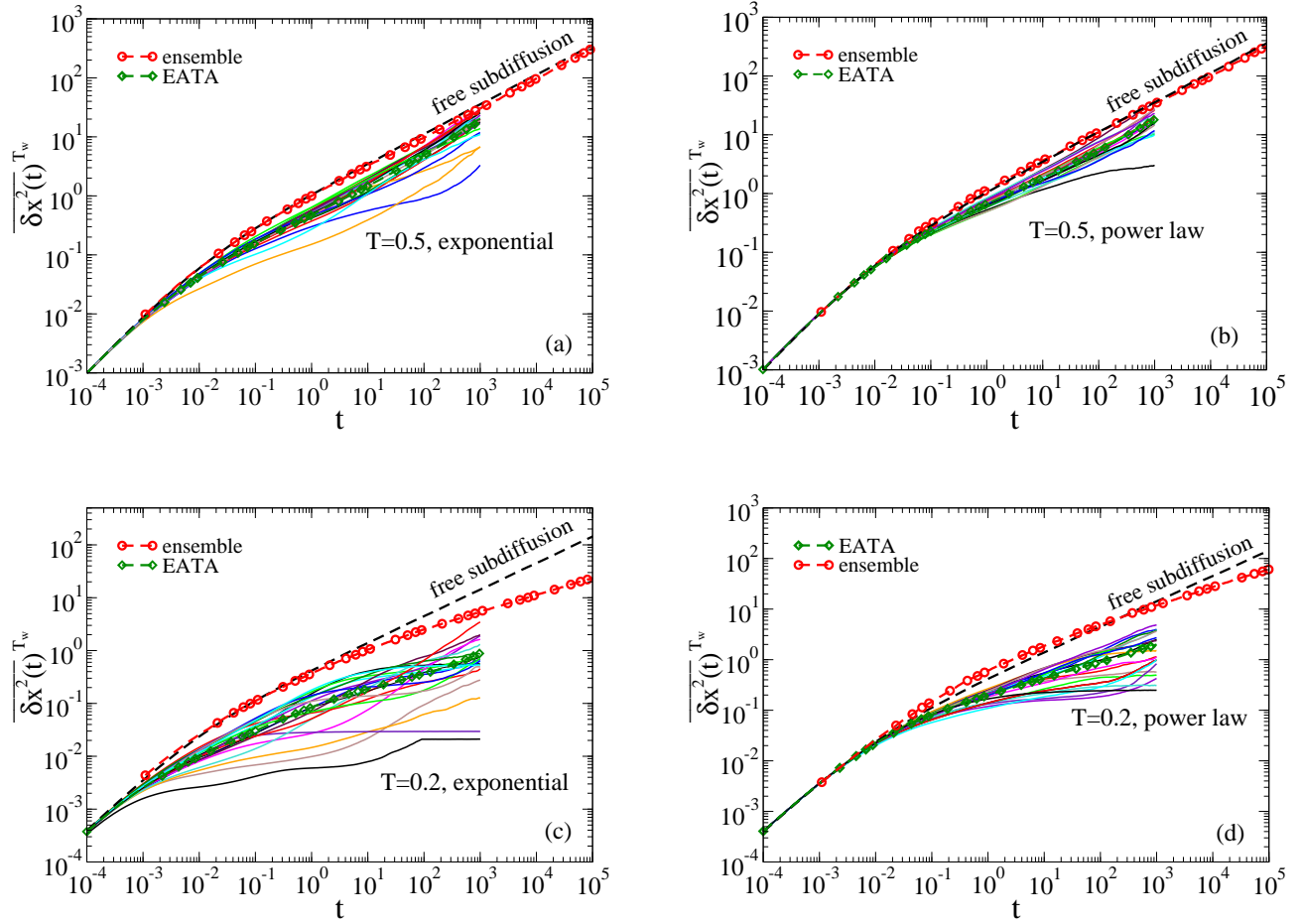


FIG. 4. (Color online) Single-trajectory, time-averaged mean squared displacement for two values of temperature $T = 0.5$ and $T = 0.2$, and two types of correlations shown in each panel. The trajectories time length was $T_w = 10^5$. 20 trajectory averages were made for particles starting from different locations. They are depicted with solid lines. The results of the ensemble-averaged, as well as ensemble-averaged time-averaged (EATA), and potential-free subdiffusion are also depicted for comparison. Remarkably, the ensemble average is only slightly suppressed by the random potential even for $T = 0.2$ in the case of power law correlations at the end point of simulations, see in the panel d, whereas transiently it is even faster. However, single-trajectory averages are suppressed essentially stronger. Generally, scatter in single-trajectory averages is visibly stronger for exponential correlations.

on the pathway and the fact that this barrier scales as $\delta U_{\max} \sim 2\sigma\sqrt{2\ln(x/x_{\text{in}})}$ [117, 128, 129] with distance, see Ref. [117] for detail in the case of normal diffusion in stationary random potentials. This scaling argumentation holds also for viscoelastic subdiffusion because a typical mean time to overcome a potential barrier scales also in Arrhenius manner with its height [10, 60], and namely this kind of behavior dominates in the transient regime, where the influence of potential on viscoelastic subdiffusion is very essential. Sinai diffusion in Eq. (6) just follows from Eq. (7) as the lowest order expansion in $k_B T/\sigma_{\text{eff}}$. The fitted values of σ_{eff} agree actually fairly good with the theoretical value $\sigma_{\text{eff}} = 2\sqrt{2} \approx 2.83\sigma$ [117]. The agreement of the fitted values with theoretical value of $x_{\text{in}} = \pi\lambda/\sqrt{\gamma} \approx 3.51\lambda$ for $\gamma = 0.8$ [117] is also rather good for power law correlated potentials, see especially for $T = 0.2$. For singular model with exponential corre-

lations, which predicts $x_{\text{in}} = \pi\sqrt{\lambda\Delta x/2} \approx 0.315\sqrt{\lambda}$ for $\Delta x = 0.02$, the agreement becomes worse. Nevertheless, scaling argumentation of Refs. [3, 117] works surprisingly good, given its very rough character, also for viscoelastic subdiffusion in random potentials. Notice that in power-law correlated potentials Sinai-like subdiffusion is essentially faster in absolute terms than one in exponentially correlated potentials. The reason becomes immediately clear from Fig. 1. This is because power-law correlated disorder is much smoother, and the maximal barrier met on the same distance is essentially smaller than in the case of exponential correlations. Furthermore, an interesting transient effect on the ensemble level is that viscoelastic subdiffusion in random potential can be even faster than free subdiffusion, see for power law correlations and $T = 0.1$ in Fig. 2, b. This is because of an alternating local bias felt by each separate particle [117]. Such a local bias and drift are responsible e.g. for the

Golosov phenomenon in the case of genuine Sinai diffusion [3, 130]. Single-trajectory averages, see below, do not show such a paradoxical feature. Then, subdiffusion is always suppressed by random potential.

An alternative to Eq. (7) way to represent the results is to introduce a time-dependent exponent $\alpha(t)$ of power-law subdiffusion

$$\langle \delta x^2(t) \rangle \approx x_{\text{in}}^2 [t/t_0]^{\alpha(t)}. \quad (8)$$

Its behavior is depicted Fig. 3. For Sinai-like diffusion at $T = 0.1$ and $T = 0.2$, $\alpha(t)$ declines in time. It should reach a minimum [117] and then logarithmically slow grow, $\alpha(t) \propto \log(t)$, as Eq. (7) predicts [117]. For $T = 0.2$ and exponential correlations, the minimum is indeed reached at $\alpha_{\text{min}} \approx 0.32$ in Fig. 3, a, which is approximately the same value as for normal diffusion in this potential [117]. The regime of logarithmically growing $\alpha(t)$ is, however, numerically practically not achievable in our simulations for $T = 0.1$ and $T = 0.2$, whereas for $T = 0.5$ it simply does not show up because the influence random potential in this case is weak. This behavior is in contrast with normal diffusion features in the studied random potentials [117].

B. Single-trajectory averages

Single-trajectory averages [11, 21, 92, 93]

$$\overline{\delta x^2(t)}^{\mathcal{T}_w} = \frac{1}{\mathcal{T}_w - t} \int_0^{\mathcal{T}_w - t} [\delta x(t|t')]^2 dt' \quad (9)$$

of the mean-squared displacement $\delta x(t|t') = x(t+t') - x(t')$ over the maximal time window \mathcal{T}_w also present interest, especially for experimentalists who often simply do not have a possibility to deal with macroscopically many particles. To avoid a trivial statistical scatter in Eq. (9), the maximal time t should be much smaller than \mathcal{T}_w . In the numerical results depicted in Fig. 4 it is just 1%. Remarkably, even for $T = 0.5$ the scatter in single-trajectory averages is strong. It is clearly more pronounced in the case of exponential correlations for the reason, which is already obvious. Notice that while the ensemble-average of single-trajectory averages, EATA, in this figure gradually converges to the ensemble-averaged result, in the case $T = 0.5$, some of the single-trajectory averages can look yet very different. In this respect, one should mention that many experimental data on subdiffusion in living cells using several strict criteria seem to clearly point out on the viscoelastic mechanism of this subdiffusion [25, 33, 37, 131]. However, other researchers doubt it because single trajectory averages reveal essential non-ergodic features [35, 36]. A tentative resolution of this paradox is that the discussed biologically related anomalous diffusion is viscoelastic subdiffusion in a random, inhomogeneous and fluctuating environment. It seems almost obvious. Differently from [35], we model this fact by imposing a random potential on viscoelastic

subdiffusion, rather than subordinating physical time to a random clock of CTRW. Indeed a typical mesh size of random actin meshwork in cytosol and model polymeric fluids is $0.1 \div 1 \mu\text{m}$ depending on the actin concentration [30]. Let us take it to be $\lambda \approx 0.308 \mu\text{m}$ and associate it with the correlation length of random potential. Furthermore, let us consider diffusion of globular proteins of the radius $R = 2.5 \text{ nm}$ (a typical one) in such a system. Actin meshwork is charged and globular proteins are also typically charged. This will cause a screened (by mobile ions) electrostatic interaction. The strength can be variable depending on the mesh size, the screening length, and the size of particle. However, $\sigma = (2 \div 5) k_B T$ can serve as a reasonable first guess in our estimate. The subdiffusion coefficient of a particle of this size in cytosol should be about the same as for a gold nanoparticle of the same radius in HeLa cells in Ref. [24]. It is estimated to be $D_\alpha \approx 0.644 \mu\text{m}^2/\text{s}^{1/2}$ in our notations (see Table I in [132]). The inertial effects in such a case are completely negligible and the time scale parameter τ_r is estimated to be $\tau_r \approx 5.48 \text{ ms}$, see in Appendix A. Hence, the maximal time in our Fig. 4 is about 5.48 s for single trajectory averages. In accordance with our results, for $\sigma = 2 k_B T$ they would be broadly scattered on this time scale as in Fig. 4, a, b, even if the averaging time window \mathcal{T}_w would be 548 s long. However, the ensemble average would be almost independent of the presence of random potential, like in Fig. 2 for $T = 0.5$. This is a first crude idea to resolve current controversies. However, a further quantitative analysis of the available experimental data from the discussed perspective of viscoelastic subdiffusion in random potentials is required.

C. Escape time distribution

The success of the scaling argumentation extended from normal to subdiffusive viscoelastic dynamics in stationary Gaussian potentials suggests that the escape time distributions should also be similar. We consider escape of the particles out of $[-\lambda, \lambda]$ spatial interval, which are initially located at its center. The distribution of logarithmically transformed escape times, $z = \ln t$, is plotted in Fig. 5. Indeed, a generalized log-normal distribution of Ref. [117]

$$\psi(t) = \frac{C}{t} \left[e^{-|\ln(t/t_m)/\kappa_1|^{b_1}} \theta(t_m - t) + e^{-|\ln(t/t_m)/\kappa_2|^{b_2}} \theta(t - t_m) \right], \quad (10)$$

where $C = b_1 b_2 / [b_2 \kappa_1 \Gamma(1/b_1) + b_1 \kappa_2 \Gamma(1/b_2)]$ is a normalization constant, $b_{1,2} > 1$, and $\kappa_{1,2} > 0$, fits excellently to the numerical data for the both considered models of correlations. General features are similar to those of memoryless diffusion. The escape density has a maximum at $\ln t_m$ value of the logarithmically transformed time variable. Furthermore, escape in the power-law correlated potentials occurs much faster than in the exponentially

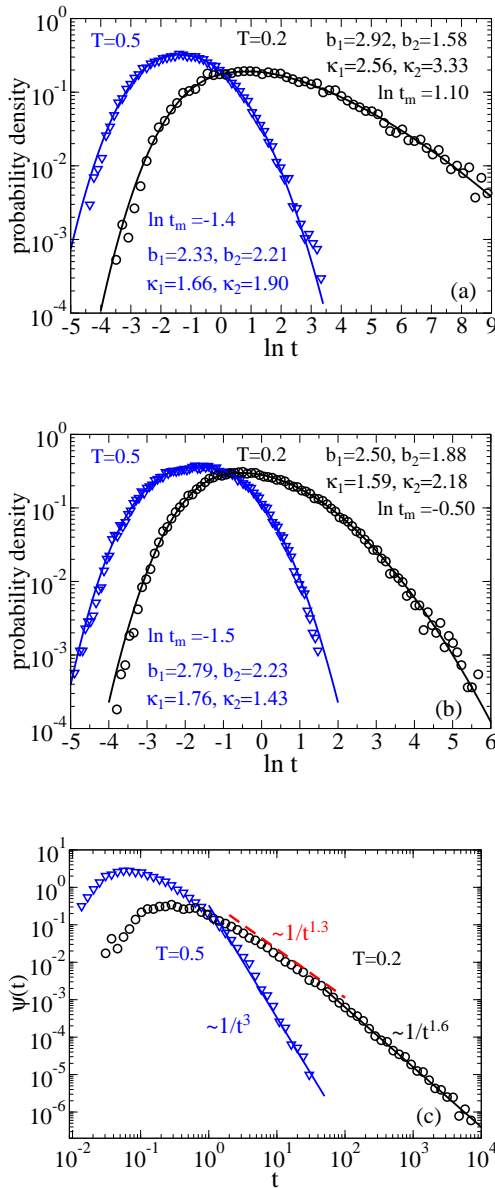


FIG. 5. (Color online) Probability density function of log-transformed first escape times, $z = \ln t$, from the interval $[-\lambda, \lambda]$ for two temperatures $T = 0.5$ (in blue) and $T = 0.2$ (in black). The cases in the different panels are: (a) exponential correlations, (b) power-law correlations with $\gamma = 0.8$. The symbols represent simulations data, the lines correspond to a fit with the probability density (10). Parameters are shown in the panels. With decreasing temperature the distributions become broader and the parameter b_2 smaller. In (c), probability densities of the original non-transformed time variable are plotted which correspond to the part (a). In this case, $\psi(t)$ seems to show some parts with power law dependencies. Especially confusing is the case of $T = 0.2$, where the part of distribution with negative exponent -1.3 (indicated in red), in a conjunction with $\alpha(t) \approx \alpha_{\min} \approx 0.32$ in Fig. 3, a and broad scatter of single trajectory averages in Fig. 4, c can be erroneously interpreted within a CTRW theory with divergent mean residence time.

correlated potentials. The exponent b_2 is strongly temperature dependent. With lowering temperature it becomes smaller and closer to one. However, all the moments of RTD remain finite. Notice that this generalized log-normal distribution can sometimes be easily mistaken for a power law, if to plot it in doubly logarithmic coordinates for the original non-transformed time variable as e.g. in Fig. 5, c, in the case of exponential correlations. This is why to know the moments of experimental distributions is important, as well as using other representations of experimental data, upon a transformation of random variable, like in our Fig. 5, a, b. This would allow a new look on the existing experimental data in the light of our model. Indeed, it is very tempting to interpret $\psi(t) \propto 1/t^{1.3}$ in Fig. 5, c for $T = 0.2$ in conjunction with $\alpha(t) \approx \alpha_{\min} \approx 0.32$ in Fig. 3, a, and a strong scatter of single-trajectory averages in Fig. 4, c within the traditional CTRW theory with divergent mean residence time. However, real physics in this particular case is very different.

IV. SUMMARY AND CONCLUSIONS

In this work we studied numerically viscoelastic subdiffusion governed by fractional Langevin equation in stationary Gaussian random potentials for several models of decaying correlations. Our study revealed several surprises. First of all, on the ensemble level the influence of random potential is almost completely negligible for $\sigma = k_B T$. Viscoelastic subdiffusion easily wins over the potential randomness, even if the potential is wildly fluctuating as in the case of exponentially decaying correlation, see in Fig. 1. This is a very unexpected result because (i) normal diffusion in such potentials is suppressed by the factor $\exp[-(\sigma/k_B T)^2]$ which is approximately 0.368 in this case, (ii) slowness combined with sluggishness intuitively should result into a super-slowness. However, this intuition fails completely. Nevertheless, this surprising result was already partially anticipated in view of akin influence of the periodic potentials on viscoelastic subdiffusion [10, 60]. It has precisely the same explanation: Distributions of the escape times out of metastable minima have finite moments, and the asymptotic behavior is determined by viscoelastic long-time correlations in the medium that yield unobstructed subdiffusion. With the increase of the disorder strength to $\sigma = 2k_B T$, the presence of a transient behavior becomes slightly visible. However, on the ensemble level the effect is really weak and one can clearly deduce from numerics that the asymptotic regime is almost achieved at the end of our simulations. At odds with $\exp[-(\sigma/k_B T)^2] \approx 0.018$ for normal diffusion in this case, viscoelastic subdiffusion is practically not suppressed at all. Nevertheless, in spite of a barely noticeable effect on the ensemble level, single-trajectory averages can exhibit substantial scatter. This might provide a key insight to understand some experiments on subdiffusion in biologi-

cal cells, which typically can be viscoelastic subdiffusion in a random environment, what naturally leads to the model we considered. With a further increase of randomness strength to $\sigma \sim (5 \div 10)k_B T$, a very distinct behavior emerges. For $\sigma = 10 k_B T$, it is clearly Sinai subdiffusion, $\langle \delta x^2(t) \rangle \propto \ln^4(t)$, for both exponential and power law correlations. Its origin can be explain in a very similar manner as in the case of normal diffusion in such potentials. It is caused by extremal value fluctuations of the potential $\delta U_{\max}(x) \propto \sqrt{\ln x}$ and has clearly a transient character. Ultimately, the regime of potential-free viscoelastic subdiffusion will be reached. However, the transients can last so long that they never will be reached in reality. For an intermediate $\sigma = 5 k_B T$, a more complex behavior in Eq. (7) substantiate, in agreement with numerics, the reasoning based on a scaling argumentation [117] and Arrhenius character of viscoelastic diffusion over potential barriers [60].

The author is confident that these highly surprising results will attract attention of both theorists and experimentalists leading to a further research in this currently least explored area of anomalous diffusion.

ACKNOWLEDGMENT

Funding of this research by the Deutsche Forschungsgemeinschaft (German Research Foundation), Grant GO 2052/3-1 is gratefully acknowledged.

Appendix A: Velocity autocorrelation function for nanoparticles in viscoelastic media and neglection of inertial effects

In this Appendix, a justification of the neglection of inertial effects is given. For free viscoelastic subdiffusion with the inertial effects included, the normalized stationary velocity autocorrelation function (VACF) in the Laplace space reads, see Eq. (B26) in Ref. [10] or Eq. (A3) in Ref. [60],

$$\tilde{K}_v(s) = \frac{1}{s + \tilde{\eta}(s)/m}, \quad (\text{A1})$$

where $\tilde{\eta}(s)$ is Laplace-transform of a general memory kernel and m is the mass of particles. For the memory kernel in this paper it is

$$\tilde{K}_v(s) = \frac{1}{s + \gamma_0 + \gamma_\alpha s^{\alpha-1}}, \quad (\text{A2})$$

where $\gamma_0 = \eta_0/m$ and $\gamma_\alpha = \eta_\alpha/m$. In this case, $\int_0^\infty K_v(t)dt = 0$, for any $\eta_\alpha \neq 0$. For normal diffusion with $\eta_\alpha = 0$, $K_v(t) = \exp(-t/\tau_v^{(0)})$, in the time domain, where $\tau_v^{(0)} = m/\eta_0$ the velocity relaxation constant. For the case of purely fractional friction with $\eta_0 = 0$, $K_v(t) = E_{2-\alpha}[-(t/\tau_v)^{2-\alpha}]$ [10, 72], where

$E_\alpha(z) = E_{\alpha,b=1}(z)$ is the Mittag-Leffler function, and $\tau_v = (m/\eta_\alpha)^{1/(2-\alpha)}$ is the velocity relaxation constant of anomalous relaxation, which has in this case a negative power-law tail, $K_v(t) \propto -1/(t/\tau_v)^{2-\alpha}$, for $t \gg \tau_v$. Notice, that in both cases the velocity relaxation is instant in the strict limit $m \rightarrow 0$. This limit is singular because the mean-square thermal velocity diverges $v_T^2 = k_B T/m \rightarrow \infty$. This the reason why both the normal Brownian motion (Wiener process) and fBm are not differentiable, being singular processes in this respect, though of wide and common use in physics. Furthermore, after some lengthy algebra one obtains the following exact result in the case $\alpha = 1/2$:

$$K_v(t) = \sum_{i=1}^3 c_i z_i^2 \exp(z_i^2 t/\tau_v) \operatorname{erfc}(z_i \sqrt{t/\tau_v}) \quad (\text{A3})$$

where $\tau_v = (m/\eta_\alpha)^{2/3}$,

$$z_1 = \frac{2}{3 \cdot 4^{1/3}} \frac{\gamma_0 \tau_v}{(\sqrt{1 + 12(\gamma_0 \tau_v)^3/81} - 1)^{1/3}} - \frac{4^{1/3}}{2} (\sqrt{1 + 12(\gamma_0 \tau_v)^3/81} - 1)^{1/3}, \quad (\text{A4})$$

$$z_{2,3} = -z_1/2 \pm i \frac{\sqrt{3}}{2} \times \left[\frac{4^{1/3}}{2} (\sqrt{1 + 12(\gamma_0 \tau_v)^3/81} - 1)^{1/3} + \frac{2}{3 \cdot 4^{1/3}} \frac{\gamma_0 \tau_v}{(\sqrt{1 + 12(\gamma_0 \tau_v)^3/81} - 1)^{1/3}} \right] \quad (\text{A5})$$

and

$$c_1 = \frac{1}{(z_1 - z_2)(z_1 - z_3)},$$

$$c_2 = \frac{1}{(z_1 - z_2)(z_3 - z_2)},$$

$$c_3 = \frac{1}{(z_2 - z_3)(z_1 - z_3)}. \quad (\text{A6})$$

For $\gamma_0 = 0$, $z_1 = 1$ and $z_{2,3} = -1/2 \pm i\sqrt{3}/2$. Independently of γ_0 , the asymptotics reads

$$K_v(t) \sim -\frac{1}{2\sqrt{\pi}(t/\tau_v)^{3/2}} \quad (\text{A7})$$

for $t \gg \tau_v$. Notice that already for $t > 100\tau_v$, $K_v(t)$ is really small and the overdamped approximation can be accurately used, on theoretical grounds. In fact, however, the initial ballistic regime is already over for $t > (3 \div 5)\tau_v$ in reality, see e. g. Figs. 5, 6 in [10]. It is important to emphasize that this fact does not contradict to another fact that double integration of $v_T^2 K_v(t)$ yields the mean square displacement whose behavior is determined by the discussed tail and where the time scale τ_v drops out. This important time scale defines the initial ballistic regime, see in Refs. [60], [10] which is of no importance in this work. For $0 \leq \gamma_0 \tau_v < \gamma_0^{(c)} \tau_v \approx 0.220404$, $K_v(t)$ changes

its sign precisely three times. For a larger $\gamma_0\tau_v$, a single change of the sign occurs.

Let us estimate now the time scale τ_v of the velocity relaxation for diffusion of nanoparticles in viscoelastic cytosol of living cells. For the colloidal gold particles with radius $R = 2.5$ nm in [24] subdiffusion was found in HeLa cells with $\alpha \approx 0.51 \approx 0.5$ and $D_\alpha \approx 0.644 \mu\text{m}^2/\text{s}^\alpha$ (see in Table I in [132]) on the time scale up to 1 s, at least. Let us use this experimental value and the generalized Einstein relation $D_\alpha = k_B T / \eta_\alpha$ to estimate $\tau_v = (4\pi\rho R^3 D_{1/2} / (3k_B T))^{2/3}$, where ρ is the mass density of particle. With the gold mass density $\rho = 19.3 \text{ kg/m}^3$ and room $k_B T = 4.1 \text{ pN} \cdot \text{nm}$, we obtain $\tau_v \approx 28.08$ ps (picoseconds!). For lighter particles such as globular proteins with $\rho \sim 1.2 \text{ kg/m}^3$ it will be even smaller. Thus, already on the time scale of nanoseconds and larger the inertial effects are completely negligible, for sure. Furthermore, the normal diffusion coefficient D_0 in the water component of cytosol can be estimated us-

ing the Einstein-Stokes relation as $D_0 = k_B T / (6\pi\zeta_w R)$, where $\zeta_w \approx 1 \text{ mPa} \cdot \text{s}$ is water viscosity. This yields $D_0 \approx 87 \mu\text{m}^2/\text{s}$. The corresponding time τ_0 separating the initially normal diffusion and subdiffusion in our paper is hence $\tau_0 = (D_{1/2}/D_0)^2 \approx 54.77 \mu\text{s}$. It is of the order 10^6 larger than τ_v , which once again confirms that the inertial effects are completely negligible. In fact, the time step in our numerical simulations exceeds this estimated τ_v by orders of magnitude. Furthermore, the scaling time τ_r used in simulations can be expressed for $\alpha = 1/2$ via dimensionless $\tilde{\eta}_0$ as $\tau_r = \tau_0 / \tilde{\eta}_0^2$, which for $\tilde{\eta}_0 = 0.1$ used in numerics gives $\tau_r = 100\tau_0 \approx 5.48 \text{ ms}$. Hence, the maximal time $t_{\text{max}} = 2 \times 10^5$ in our numerics corresponds to about $t_{\text{max}} = 1096 \text{ s}$. The corresponding length scale, which we took to be the correlation scale, is estimated as $\lambda = \tau_r^{1/4} (D_{1/2}\sigma / k_B T)^{1/2} \approx 0.218 \sqrt{\sigma / k_B T} \mu\text{m}$, i.e. $\lambda \approx 0.308 \mu\text{m}$ for $\sigma = 2$ (in units of $k_B T$), or $\lambda \approx 0.689 \mu\text{m}$ for $\sigma = 10$, which are typical mesh sizes in random actin meshworks [30].

-
- [1] M. F. Shlesinger, J. Stat. Phys. **10**, 421 (1974).
 - [2] H. Scher and E. W. Montroll, Phys. Rev. B **12**, 2455 (1975).
 - [3] J.-P. Bouchaud and A. Georges, Phys. Rep. **195**, 127 (1990).
 - [4] D. ben Avraham and S. Havlin, *Diffusion and Reactions in Fractals and Disordered Systems* (Cambridge University Press, Cambridge, 2000).
 - [5] B. D. Hughes, *Random Walks and Random Environments* (Clarendon Press, Oxford, 1995).
 - [6] J. Bouchaud, A. Comtet, A. Georges, and P. L. Doussal, Ann. Phys. (N.Y.) **201**, 285 (1990).
 - [7] J. P. Bouchaud, J. Phys. I (Paris) **2**, 1705 (1992).
 - [8] R. Metzler and J. Klafter, Phys. Rep. **339**, 1 (2000).
 - [9] J. Klafter, S. C. Lim, and R. Metzler, eds., *Fractional Dynamics: Recent Advances* (World Scientific, New Jersey, 2011).
 - [10] I. Goychuk, Adv. Chem. Phys. **50**, 187 (2012).
 - [11] R. Metzler, J.-H. Jeon, A. G. Cherstvy, and E. Barkai, Phys. Chem. Chem. Phys. **16**, 24128 (2014).
 - [12] T. G. Mason and D. A. Weitz, Phys. Rev. Lett. **74**, 1250 (1995).
 - [13] F. Amblard, A. C. Maggs, B. Yurke, A. N. Pargellis, and S. Leibler, Phys. Rev. Lett. **77**, 4470 (1996).
 - [14] M. J. Saxton and K. Jacobsen, Ann. Rev. Biophys. Biomolec. Struc. **26**, 373 (1997).
 - [15] T. A. Waigh, Rep. Progr. Phys. **68**, 685 (2005).
 - [16] G. Seisenberger, M. U. Ried, T. Endress, H. Büning, M. Hallek, and C. Bräuchle, Science **294**, 1929 (2001).
 - [17] A. Caspi, R. Granek, and M. Elbaum, Phys. Rev. E **66**, 011916 (2002).
 - [18] M. Weiss, M. Elsner, F. Kartberg, and T. Nilsson, Biophys. J. **87**, 3518 (2004).
 - [19] I. M. Tolic-Norrelykke, E.-L. Munteanu, G. Thon, L. Oddershede, and K. Berg-Sorensen, Phys. Rev. Lett. **93**, 078102 (2004).
 - [20] D. S. Banks and C. Fradin, Biophys. J. **89**, 2960 (2005).
 - [21] E. Barkai, Y. Garini, and R. Metzler, Phys. Today **65** (8), 29 (2012).
 - [22] L. Bruno, M. Salierno, D. E. Wetzler, M. A. Desposito, and V. Levi, PLoS ONE **6**, e18332 (2011); L. Bruno, V. Levi, M. Brunstein, and M. A. Desposito, Phys. Rev. E **80**, 011912 (2009).
 - [23] I. Golding and E. C. Cox, Phys. Rev. Lett. **96**, 098102 (2006).
 - [24] G. Guigas, C. Kalla, and M. Weiss, Biophys. J. **93**, 316 (2007).
 - [25] J. Szymanski and M. Weiss, Phys. Rev. Lett. **103**, 038102 (2009).
 - [26] F. Höfling and T. Franosch, Rep. Prog. Phys. **76**, 046602 (2013).
 - [27] J. H. Jeon, V. Tejedor, S. Burov, E. Barkai, C. Selhuber-Unkel, K. Berg-Sørensen, L. Oddershede, and R. Metzler, Phys. Rev. Lett. **106**, 048103 (2011).
 - [28] K. Luby-Phelps, Mol. Biol. Cell **24**, 2593 (2013).
 - [29] W. Pan, L. Filobelo, N. D. Q. Pham, O. Galkin, V. V. Uzunova, and P. G. Vekilov, Phys. Rev. Lett. **102**, 058101 (2009).
 - [30] I. Y. Wong, M. L. Gardel, D. R. Reichman, E. R. Weeks, M. T. Valentine, A. R. Bausch, and D. A. Weitz, Phys. Rev. Lett. **92**, 178101 (2004).
 - [31] A. W. Harrison, D. A. Kenwright, T. A. Waigh, P. G. Woodman, and V. J. Allan, Phys. Biol. **10**, 036002 (2013).
 - [32] B. R. Parry, I. V. Surovtsev, M. T. Cabeen, C. S. O'Hern, E. R. Dufresne, and C. Jacobs-Wagner, Cell **156**, 183 (2014).
 - [33] D. Robert, T.-H. Nguyen, F. Gallet, and C. Wilhelm, PLoS ONE **4**, e10046 (2010).
 - [34] I. Goychuk, V. O. Kharchenko, and R. Metzler, PLoS ONE **9**, e91700 (2014); Phys. Chem. Chem. Phys. **16**, 16524 (2014); I. Goychuk, Phys. Biol. **12**, 016013 (2015).
 - [35] S. M. A. Tabei, S. Burov, H. Y. Kima, A. Kuznetsov, T. Huynha, J. Jureller, L. H. Philipson, A. R. Dinner, and N. F. Scherer,

- Proc. Natl. Acad. Sci. (USA) **110**, 4911 (2013).
- [36] A. V. Weigel, B. Simon, M. M. Tamkun, and D. Krapf, Proc. Natl. Acad. Sci. (USA) **108**, 6438 (2011).
- [37] M. Weiss, Phys. Rev. E **88**, 010101 (2013).
- [38] I. Santamaria-Holek, J. M. Rubi, and A. Gadomski, J. Phys. Chem. B **111**, 2293 (2007).
- [39] E. Bertseva, D. Grebenkov, P. Schmidhauser, S. Gribkova, S. Jeney, and L. Forro, Eur. Phys. J. E **35**, 63 (2012).
- [40] F. Evers, R. D. L. Hanes, C. Zunke, R. F. Capellmann, J. Bewerunge, C. Dalle-Ferrier, M. C. Jenkins, I. Ladadwa, A. Heuer, R. Castaneda-Priego, and S. U. Egelhaaf, Eur. Phys. J. Spec. Top. **222**, 2995 (2013).
- [41] R. D. L. Hanes, M. Schmiedeberg, and S. U. Egelhaaf, Phys. Rev. E **88**, 062133 (2013).
- [42] S. Nunomura, D. Samsonov, S. Zhdanov, and G. Morfill, Phys. Rev. Lett. **96**, 015003 (2006).
- [43] M. Schubert, E. Preis, J. C. Blakesley, P. Pingel, U. Scherf, and D. Neher, Phys. Rev. B **87**, 024203 (2013).
- [44] H. Yang, G. Luo, P. Karnchanaphanurach, T.-M. Louie, I. Rech, S. Cova, L. Xun, and X. S. Xie, Science **302**, 262 (2003).
- [45] S. C. Kou and X. S. Xie, Phys. Rev. Lett. **93**, 180603 (2004).
- [46] I. Goychuk and P. Hänggi, Phys. Rev. E **70**, 051915 (2004).
- [47] G. R. Kneller and K. Hinsén, J. Chem. Phys. **121**, 10278 (2004).
- [48] W. Min, G. Luo, B. J. Cherayil, S. C. Kou, and X. S. Xie, Phys. Rev. Lett. **94**, 198302 (2005).
- [49] V. Calandrini, D. Abergel, and G. R. Kneller, J. Chem. Phys. **133**, 145101 (2010); P. A. Calligari, V. Calandrini, G. R. Kneller, and D. Abergel, J. Phys. Chem. B **115**, 12370 (2011); P. A. Calligari, V. Calandrini, J. Ollivier, J.-B. Artero, M. Härtlein, M. Johnson, and G. R. Kneller, **119**, 7860 (2015).
- [50] I. Goychuk, Phys. Rev. E **92**, 042711 (2015).
- [51] X. Hu, L. Hong, M. D. Smith, T. Neusius, X. Cheng, and J. C. Smith, Nat. Phys. **12**, 171 (2016).
- [52] G. R. Kneller, K. Baczynski, and M. Pasenkiewicz-Gierula, J. Chem. Phys. **135**, 141105 (2011).
- [53] J.-H. Jeon, H. M.-S. Monne, M. Javanainen, and R. Metzler, Phys. Rev. Lett. **109**, 188103 (2012).
- [54] J.-H. Jeon, M. Javanainen, H. Martinez-Seara, R. Metzler, and I. Vattulainen, Phys. Rev. X **6**, 021006 (2016).
- [55] M. Kong, L. Liu, X. Chen, K. I. Driscoll, P. Mao, S. Böhm, N. M. Kad, S. C. Watkins, K. A. Bernstein, J. J. Wyrick, J.-H. Min, and B. V. Houten, Mol. Cel. **64**, 376 (2016); M. Kong and B. V. Houten, Prog. Biophys. Mol. Biol. **127**, 93 (2017); L. Liu, M. Kong, N. R. Gassman, B. D. Freudentha, R. Prasad, S. Zhen, S. C. Watkins, S. H. Wilson, and B. V. Houten, Nucl. Acid. Res. **45**, 12834 (2017).
- [56] I. Goychuk and P. Hänggi, in *Fractional Dynamics: Recent Advances*, edited by J. Klafter, S. C. Lim, and R. Metzler (World Scientific, Hoboken, NJ, 2011) Chap. 13, pp. 305–327.
- [57] U. Weiss, *Quantum Dissipative Systems*, 2nd ed. (World Scientific, Singapore, 1999).
- [58] N. Pottier, Physica A **317**, 371 (2003).
- [59] R. Kupferman, J. Stat. Phys. **114**, 291 (2004).
- [60] I. Goychuk, Phys. Rev. E **80**, 046125 (2009).
- [61] I. Goychuk, E. Heinsalu, M. Patriarca, G. Schmid, and P. Hänggi, Phys. Rev. E **73**, 020101 (R) (2006); E. Heinsalu, M. Patriarca, I. Goychuk, G. Schmid, and P. Hänggi, Phys. Rev. E **73**, 046133 (2006).
- [62] F. Barbi, M. Bologna, and P. Grigolini, Phys. Rev. Lett. **95**, 220601 (2005).
- [63] I. M. Sokolov and J. Klafter, Phys. Rev. Lett. **97**, 140602 (2006).
- [64] E. Heinsalu, M. Patriarca, I. Goychuk, and P. Hänggi, Phys. Rev. Lett. **99**, 120602 (2007); Phys. Rev. E **79**, 041137 (2009).
- [65] I. Goychuk, Phys. Rev. E **76**, 040102 (R) (2007).
- [66] I. Goychuk, Comm. Theor. Phys. **62**, 497 (2014).
- [67] N. N. Bogolyubov, *On some Statistical Methods in Mathematical Physics* (Ukrainian Academy of Sciences, Kiev, 1945) pp. 115–137, (in Russian).
- [68] G. W. Ford, M. Kac, and P. Mazur, J. Math. Phys. **6**, 504 (1965).
- [69] R. Kubo, Rep. Prog. Theor. Phys. **29**, 255 (1966).
- [70] R. Zwanzig, J. Stat. Phys. **9**, 215 (1973).
- [71] K. G. Wang and M. Tokuyama, Physica A **265**, 341 (1999).
- [72] E. Lutz, Phys. Rev. E **64**, 051106 (2001).
- [73] I. Goychuk and P. Hänggi, Phys. Rev. Lett. **99**, 200601 (2007).
- [74] K. Lindenberg and V. Seshardi, Physica A **109**, 483 (1981).
- [75] G. W. Ford, J. T. Lewis, and R. F. O’Connell, Phys. Rev. A **37**, 4419 (1988).
- [76] B. J. Alder and T. E. Wainwright, J. Chem. Phys. **27**, 1208 (1957).
- [77] B. J. Alder and T. E. Wainwright, Phys. Rev. Lett. **18**, 988 (1967).
- [78] V. B. Magalinskii, Soviet Phys. JETP **9**, 1381 (1959).
- [79] A. Caldeira and A. Leggett, Ann. Phys. **149**, 374 (1983).
- [80] F. Mainardi and P. Pironi, Extracta Mathematicae **10**, 140 (1996).
- [81] M. Caputo, Geophys. J. R. Astr. Soc. **13**, 529 (1967).
- [82] R. Gorenflo and F. Mainardi, in *Fractal and Fractal Calculus in Continuum Mechanics*, edited by A. Carpinteri and F. Mainardi (Springer, Wien, 1997) pp. 223–276.
- [83] B. Mandelbrot and J. van Ness, SIAM Rev. **10**, 422 (1968).
- [84] P. Siegle, I. Goychuk, and P. Hänggi, EPL **93**, 20002 (2011).
- [85] L. D. Landau and E. M. Lifshitz, *Fluid Mechanics*, 2nd ed. (Pergamon Press, Oxford, 1987).
- [86] R. Huang, I. Chavez, K. M. Taute, B. Lukic, S. Jeney, M. G. Raizen, and E.-L. Florin, Nat. Phys. **7**, 576 (2011).
- [87] T. Franosch, M. Grimm, M. Belushkin, F. M. Mor, G. Foffi, L. Forro, and S. Jeney, Nature (London) **478**, 85 (2011).
- [88] A. N. Kolmogorov, Dokl. Akad. Nauk SSSR **26**, 115 (1940); in *Selected Works of A. N. Kolmogorov, vol. I, Mechanics and Mathematics*, edited by V. M. Tikhomirov (Kluwer, Dordrecht, 1991) pp. 303–307.
- [89] R. F. Grote and J. T. Hynes, J. Chem. Phys. **73**, 2715 (1980).
- [90] P. Hänggi, P. Talkner, and M. Borkovec, Rev. Mod. Phys. **62**, 251 (1990).
- [91] Y.-C. Chen and J. L. Lebowitz, Phys. Rev. B **46**, 10743 (1992).
- [92] Y. He, S. Burov, R. Metzler, and E. Barkai,

- Phys. Rev. Lett. **101**, 058101 (2008).
- [93] A. Lubelski, I. M. Sokolov, and J. Klafter, Phys. Rev. Lett. **100**, 250602 (2008).
 - [94] P. Reimann, Phys. Rep. **361**, 57 (2002).
 - [95] I. Goychuk, Chem. Phys. **375**, 450 (2010).
 - [96] I. Goychuk and V. Kharchenko, Phys. Rev. E **85**, 051131 (2012).
 - [97] I. Goychuk and V. O. Kharchenko, Math. Model. Nat. Phenom. **8**, 144 (2013).
 - [98] V. O. Kharchenko and I. Goychuk, Phys. Rev. E **87**, 052119 (2013).
 - [99] V. O. Kharchenko and I. Goychuk, New J. Phys. **14**, 043042 (2012).
 - [100] G. Bel and E. Barkai, Phys. Rev. Lett. **94**, 240602 (2005).
 - [101] I. Sokolov, E. Heinsalu, P. Hänggi, and I. Goychuk, Europhys. Lett. **86**, 30009 (2009).
 - [102] P. G. D. Gennes, J. Stat. Phys. **12**, 463 (1975).
 - [103] H. Bässler, Phys. Rev. Lett. **58**, 767 (1987).
 - [104] H. Bässler, Phys. Status Solidi B **175**, 15 (1993).
 - [105] R. Zwanzig, Proc. Natl. Acad. Sci. (USA) **85**, 2029 (1988).
 - [106] T. Hecksher, A. I. Nielsen, N. B. Olsen, and J. C. Dyre, Nat. Phys. **4**, 737 (2008).
 - [107] D. H. Dunlap, P. E. Parris, and V. M. Kenkre, Phys. Rev. Lett. **77**, 542 (1996).
 - [108] J. Bewerunge and S. U. Egelhaaf, Phys. Rev. A **93**, 013806 (2016).
 - [109] U. Gerland, J. D. Moroz, and T. Hwa, Proc. Natl. Acad. Sci. (USA) **99**, 12015 (2002).
 - [110] M. Lässig, BMC Bioinformatics **8**(Suppl. 6), S7 (2007).
 - [111] M. Slutsky, M. Kardar, and L. A. Mirny, Phys. Rev. E **69**, 061903 (2004).
 - [112] O. Bénichou, Y. Kafri, M. Sheinman, and R. Voituriez, Phys. Rev. Lett. **103**, 138102 (2009).
 - [113] I. Goychuk and V. O. Kharchenko, Phys. Rev. Lett. **113**, 100601 (2014).
 - [114] A. H. Romero and J. M. Sancho, Phys. Rev. E **58**, 2833 (1998).
 - [115] M. Khoury, A. M. Lacasta, J. M. Sancho, and K. Lindenberg, Phys. Rev. Lett. **106**, 090602 (2011).
 - [116] M. S. Simon, J. M. Sancho, and K. Lindenberg, Phys. Rev. E **88**, 062105 (2013).
 - [117] I. Goychuk, V. O. Kharchenko, and R. Metzler, Phys. Rev. E **96**, 052134 (2017).
 - [118] Y. G. Sinai, Theor. Prob. Appl. **27**, 247 (1982).
 - [119] G. Oshanin, A. Rosso, and G. Schehr, Phys. Rev. Lett. **110**, 100602 (2013).
 - [120] H.-G. Duan and X.-T. Liang, Eur. Phys. J. B **85**, 209 (2012).
 - [121] C.-K. Peng, S. V. Buldyrev, A. L. Goldberger, S. Havlin, F. Sciortino, M. Simons, and H. E. Stanley, Nature (London) **356**, 168 (1992).
 - [122] M. S. Simon, J. M. Sancho, and A. M. Lacasta, Fluct. Noise Lett. **11**, 1250026 (2012).
 - [123] S. A. McKinley, K. Yao, and M. G. Forest, J. Rheol. **53**, 1489 (2009).
 - [124] T. C. Gard, *Introduction to Stochastic Differential Equations* (Dekker, New York, 1988).
 - [125] R. G. Palmer, D. L. Stein, E. Abrahams, and P. W. Anderson, Phys. Rev. Lett. **53**, 958 (1984).
 - [126] R. G. Larson, *The Structure and Rheology of Complex Fluids* (Oxford University Press, New York, 1999).
 - [127] P. Siegle, I. Goychuk, P. Talkner, and P. Hänggi, Phys. Rev. E **81**, 011136 (2010).
 - [128] Y. C. Zhang, Phys. Rev. Lett. **56**, 2113 (1986).
 - [129] R. D. L. Hanes and S. U. Egelhaaf, Journal of Physics: Condensed Matter **24**, 464116 (2012).
 - [130] A. O. Golosov, Commun. Math. Phys. **92**, 491 (1984).
 - [131] M. Magdziarz, A. Weron, K. Burnecki, and J. Klafter, Phys. Rev. Lett. **103**, 180602 (2009).
 - [132] I. Goychuk, Phys. Rev. E **86**, 021113 (2012).